J Stat Phys (2008) 132: 1051–1069
DOI 10.1007/s10955-008-9591-2

Markov Chain Methods for Analyzing Urban Networks

D. Volchenkov · P. Blanchard

Received: 18 October 2007 / Accepted: 17 June 2008 / Published online: 16 July 2008

Abstract Complex transport networks abstracted as graphs (undirected, directed, or multi-component) can be effectively analyzed by random walks (or diffusions). We have unified many concepts into one framework and studied in details the structural and spectral properties of spatial graphs for five compact urban patterns.

Keywords Random walks · Complex networks · Traffic equilibrium

1 Introduction

Topology of urban environments can be represented by means of graphs. From Euler's time, urban design and townscape studies were the sources of inspiration for the network analysis and graph theory.

Transport networks are used to model the flow of commodity, information, viruses, opinions, or traffic along roads, streets, pipes, aqueducts, power lines, or nearly any structure which permits either the movement of vehicles or the flow of some commodity, products, goods or service. In Sect. 2, we discuss how a transport network may be represented by different graphs in accordance to the object-based, space-based, or time-based paradigms.

In particular, we explore the spatial graph representations of several compact urban patterns by random walks. Two of them are situated on islands: Manhattan (with an almost regular grid-like city plan) and the network of Venice canals (Venice stretches across 122 small islands, and the canals serve the function of roads). We have also considered two organic cities founded shortly after the Crusades and developed within the medieval fortresses: Rothenburg ob der Tauber (the medieval Bavarian city preserving its original structure from the 13th century) and the downtown of Bielefeld (Altstadt Bielefeld), an economic and cultural center of Eastern Westphalia. To supplement the study of urban canal networks, we have investigated that one in the city of Amsterdam.

D. Volchenkov (✉) · P. Blanchard
BiBoS, University Bielefeld, Postfach 100131, 33501, Bielefeld, Germany
e-mail: volchenk@physik.uni-bielefeld.de

While identifying a street (canal) over a plurality of routes on the city map, the "named-street" approach had been used, in which two different arcs of the original street (canal) network are assigned to the same street ID provided they have the same street name. The spatial graphs of the urban patterns have been constructed by mapping edges coded with the same street (canal) ID into nodes of the spatial graph, and intersections among each pair of edges in the original graph—into edges connecting the corresponding nodes.

In general, graphs do not possess the structure of Euclidean space and therefore, their structural analysis can be difficult. In Sect. 3, we show that a structure of Euclidean space can nevertheless be defined on undirected graphs by random walks (or diffusions).

In Sect. 4, we have analyzed the spectral properties of Laplace operator describing the diffusion process on the spatial graphs representing the compact urban patterns and found that the spectral densities for them are close to normal distributions.

In Sect. 5, we investigate the Laplace spectra (which are non-negative) by the method of characteristic functions strongly inspired by statistical mechanics. The mean eigenvalue (which corresponds to the internal energy in statistical mechanics), the standard deviation of eigenvalues around the mean, and the entropy allow tracks out the dramatic structural difference between organic cities gradually developed during centuries and modern cities planned in grid.

In Sect. 6, we have extended the approach developed in the previous sections to the case of directed graphs and multi-component directed graphs. The latter graphs can be considered as a number of transport networks (transportation modes) interacting with each other by means of passengers.

We conclude in the last section.

2 Transport Networks and Their Representations

The ultimate goals of network theory are to help people in planning the efficient land use, feasible logistic, expeditious energy grids, and streamlined communications. Most of the life-sustaining networks are essentially small—usually, they amount to just several hundred nodes connected by no means at random.

Systems consisting of many individual units sharing information, people, and goods have to be modified frequently to meet the natural challenges. However, due to the lack of understanding of the result between the modifications and the possible response of the entire network, it has been always difficult to make the proper decisions on how to sustain the system and to cope with the new demand. The counter-intuitive phenomenon known as the *Braess paradox* is an example [1]; it occurs when adding more resources to a transport network (say, a new road or a bridge) deteriorates the quality of traffic by creating worse delays for the drivers, rather than alleviates it. The Braess paradox has been observed in the street vehicular traffic of New York City and Stuttgart [2].

Any graph representation of a network arises when we abstract the system by eliminating all but one of its features and by grouping units sharing a common attribute into classes. Transport networks are rather complex to be seen from a single viewpoint—usually, we may introduce nodes and edges in many different ways. Indeed, a system of objects interacting in space in laps of time may be represented by different graphs in accordance to the object-based, space-based, or time-based paradigms. Let us specify them for the example of urban networks.

The object-based paradigm is originated from the famous paper of L. Euler on the seven bridges of Königsberg (1736), in which the landmasses, the city districts and individual

buildings delivering place for people and their activity, had been marked by nodes of a planar graph, while bridges had been considered as edges [3]. The usual city plan is an example of the object-based representation of the city.

The space-based paradigm of the urban network representation comes from the idea that people perceive and organize spatial information as they navigate through the city. It has been formulated in the framework of Space Syntax theory by B. Hillier and his colleagues [4, 5]. The common attribute of space is that we can move through it following a straight line-of-sight. The space of motion can be broken into components—axial lines—which are considered as nodes connected in the non-planar spatial graph by edges which represent the junctions of axial lines. Other heuristic approaches have been used in order to divide the space of motion in cities in [6–12].

Finally, the time-based representation of a network arises naturally when we are interested in how much time a pedestrian or a vehicle would spend while travelling through a particular place. The common attribute of all spaces of motion in this case is that we can spend some time while moving through them. Then the time-based representation of the city is nothing else but a queuing network [13], in which each space of motion is considered as a service station characterized by some time of service, and the relations between the segments of streets, squares, and round-abouts are traced through their junctions.

All three graph representations are essentially different even if they describe one and the same network. Therefore, a comprehensive investigation of the transport network certainly requires that all representations have to be analyzed.

The structural analysis of graphs is challenging on account of lack of a structure of Euclidean space we used to live in. Euclidean space has a decisive role in visual and motor precepts, and in hearing thus determining our spatial perception. We never see a physical image of the entire network, but only individual objects which we may recognize as nodes. While trying to understand the network, we imagine its simplified model that indeed speeds up the interpretation process, but gives rise to multiple illusions [14].

3 Analysis of Undirected Graphs by Random Walks

In [16], we have shown that a structure of Euclidean space can be nevertheless defined on undirected connected graphs in a probabilistic sense. In the present section, we formulate the random walk approach to the analysis of undirected graphs in its final form.

It is well-know (see, for example [15, Chap. 4]) that a transitive permutation group may be represented graphically, and the converse is also true: a graph gives rise to a permutation group, in its turn.

The representation of the set of graph automorphisms $\mathrm{Aut}(G)$—the mappings of the graph $G(V, E)$ (where V is the set of nodes, and E is the set of edges) to itself which preserve all of its structure—in the class of stochastic matrices is nothing else but a generalized discrete time random walk transition operator,

$$T_{ij}^{(\beta)} = (1-\beta)\delta_{ij} + \beta\frac{A_{ij}}{k_i}, \tag{1}$$

in which the graph adjacency matrix, $A_{ij} > 0$ if $i \sim j$, but $A_{ij} = 0$ otherwise, $k_i = \sum_j A_{ij}$ is the degree of the node i in $G(V, E)$, and $\beta \in]0, 1]$. In comparison with conventional random walks defined on undirected graphs discussed in [18, 19] in details, the operator (1) contains the diagonal part $(1-\beta)$, the probability that a random walker stays in the initial vertex, while it moves to another node randomly chosen among the nearest neighbors with

probability β/k_i. The stochastic process defined by (1) can therefore be regarded as "lazy" random walks, and β is the laziness parameter. The position of a walker at time t therefore depends only on its position at time $t-1$, so that the process (1) constitutes a Markov chain.

The attractiveness of random walks methods relies on the fact that any density distribution σ defined on any undirected non-bipartite graph after $t \gg 1$ steps tends to a well-defined stationary distribution $\pi = \lim_{t\to\infty} \sigma (T^{(\beta)})^t$, which is uniform if the graph is regular. It is easy to check that the stationary distribution of lazy random walks is the same as for the conventional random walks defined by $T^{(\beta=1)}$.

The transition operator establishes relations between graph nodes and eigenmodes of the diffusion process. The idea to investigate the diffusion eigenmodes in order to study the properties of a graph belongs to J.-L. Lagrange [17] who calculated the spectrum of the Laplace operator defined on a chain (a linear graph) in order to study the discretization of the acoustic equations.

It is convenient to convert these eigenmodes into an orthonormal basis $\{\psi_k\}$ of Hilbert space $\mathcal{H}(V)$ by the standard Gram-Schmidt process that is equivalent to the introduction of the self-adjoint operator,

$$\widehat{T}^{(\beta)} = \frac{1}{2}\left(\pi^{1/2} T^{(\beta)} \pi^{-1/2} + \pi^{-1/2} \left(T^{(\beta)}\right)^{\top} \pi^{1/2}\right), \tag{2}$$

where $(T^{(\beta)})^{\top}$ is the adjoint operator, and π is defined as the diagonal matrix $\mathrm{diag}(\pi_1, \ldots, \pi_N)$ of the stationary distribution, $\sum_{i\in V} \pi_i = 1$. The symmetric operator (2) for $\beta = 1$ is used for the calculation of the characteristic times such as the first passage time to the nodes in theory of random walks defined on undirected graphs (see [18, 19]).

The set of real eigenvectors $\{\psi_i\}_{i=1}^N$ of the symmetric transition operator $\widehat{T}^{(\beta)}$ belonging to the ordered eigenvalues $1 = \mu_1 > \mu_2 \geq \cdots \geq \mu_N \geq -1$ is useful for decomposing normalized functions defined on V. The components of the first eigenvector ψ_1 belonging to the largest eigenvalue $\mu_1 = 1$,

$$\psi_1 \widehat{T}^{(\beta)} = \psi_1, \qquad \psi_{1,i}^2 = \pi_i, \tag{3}$$

describe the probability to observe a random walker in $i \in V$ and is independent of β. The Euclidean norm in the orthogonal complement of ψ_1, $\sum_{s=2}^N \psi_{s,i}^2 = 1 - \pi_i$, gives the probability that a random walker is not in i. The eigenvectors, $\{\psi_s\}_{s=2}^N$, belonging to the ordered eigenvalues $1 > \mu_2 \geq \cdots \geq \mu_N \geq -1$ depend on β.

Any vector of the Euclidean space $\mathbf{v} \in \mathbb{R}^N$ can be expanded into $\mathbf{v} = \sum_{k=1}^N \langle \mathbf{v}|\psi_k\rangle\langle\psi_k|$, and since $\psi_{1,i} \equiv \sqrt{\pi_i} > 0$ for any $i \in V$, into

$$\mathbf{v}\pi^{-1/2} = \sum_{s=2}^{N} \langle \mathbf{v}|\psi'_s\rangle\langle\psi'_s|,$$

as well. Thus,

$$\psi'_s \equiv \left(1, \frac{\psi_{s,2}}{\psi_{s,1}}, \ldots, \frac{\psi_{s,N}}{\psi_{s,1}}\right), \quad s = 2, \ldots, N, \tag{4}$$

are the basis vectors of the homogeneous coordinates spanning the projective space $P\mathbb{R}_{\pi}^{(N-1)}$, the orthogonal complement to the vector associated to the stationary distribution π. It is clear that the operator $\widehat{T}^{(\beta)}|_{P\mathbb{R}_{\pi}^{(N-1)}}$ restricted to the $(N-1)$-dimensional hypersurface $\{\psi_{1,i} = \sqrt{\pi_i}\}^{\perp}$ determines a contractive discrete-time affine dynamical system on

that, for which the only fixed point is the origin represented by

$$\lim_{n\to\infty} \left(\widehat{T}^{(\beta)}\right)^n \xi = (1, 0, \ldots, 0), \tag{5}$$

in the homogeneous coordinates (4). Any point $\xi \in P\mathbb{R}_{\pi}^{(N-1)}$ (i.e., a density distribution) generates an orbit under the consecutive action of $\widehat{T}^{(\beta)}|_{P\mathbb{R}_{\pi}^{(N-1)}}$.

The dynamics of a large number of random walkers on undirected graphs can be described by the discrete Laplace operator,

$$\widehat{L}_{\beta} = \beta \widehat{L}, \tag{6}$$

and the normalized Laplace operator $\widehat{L} \equiv \mathbf{1} - \widehat{T}^{(\beta=1)}$ is well known in the spectral graph theory [20]. The eigenvectors $\{\psi_k\}$ of (6) coincide with those of $\widehat{T}^{(\beta=1)}$, and the eigenvalues are simply related as $\lambda_k = 1 - \mu_k$, where μ_k are the eigenvalues of $\widehat{T}^{(\beta=1)}$; the smallest eigenvalue is therefore $1 - \mu_1 = 0$.

The key observation is that the Laplace operator (6) restricted to $P\mathbb{R}_{\pi}^{(N-1)}$ is always invertible, and the unique inverse operator,

$$\widehat{L}_{\beta}^{-1}\big|_{P\mathbb{R}_{\pi}^{(N-1)}} = \frac{1}{\beta} \sum_{s=2}^{N} \frac{|\psi_s'\rangle\langle\psi_s'|}{\lambda_s}, \tag{7}$$

is the Green function describing long-range interactions between eigenmodes of the diffusion process induced by the graph structure. In (7), we have denoted as usual $\psi_k' \equiv \psi_k/\psi_1$, where ψ_k are the ordered eigenvectors of $\widehat{T}^{(\beta=1)}$.

It is clear from (6–7) that laziness $\beta \in]0, 1]$ is nothing else but a time rescaling parameter.

Hilbert space on $P\mathbb{R}_{\pi}^{(N-1)}$ can be defined via the scalar product between any two vectors $\xi, \zeta \in P\mathbb{R}_{\pi}^{(N-1)}$ by

$$(\xi, \zeta)_{P\mathbb{R}_{\pi}^{(N-1)}} = (\xi, \widehat{L}_{\beta}^{-1}\zeta). \tag{8}$$

The inner product (8) allows us to define the norm of the vector $\xi \in P\mathbb{R}_{\pi}^{(N-1)}$ by setting

$$\|\xi\|^2_{P\mathbb{R}_{\pi}^{(N-1)}} = (\xi, \widehat{L}_{\beta}^{-1}\xi), \tag{9}$$

and the angle between two vectors,

$$\widehat{(\xi, \zeta)} = \arccos\left(\frac{(\xi, \zeta)_{P\mathbb{R}_{\pi}^{(N-1)}}}{\|\xi\|_{P\mathbb{R}_{\pi}^{(N-1)}} \|\zeta\|_{P\mathbb{R}_{\pi}^{(N-1)}}}\right). \tag{10}$$

This Euclidean metric is naturally defined by the distance between two points,

$$\|\xi - \zeta\|^2_{P\mathbb{R}_{\pi}^{(N-1)}} = \|\xi\|^2_{P\mathbb{R}_{\pi}^{(N-1)}} + \|\zeta\|^2_{P\mathbb{R}_{\pi}^{(N-1)}} - 2(\xi, \zeta)_{P\mathbb{R}_{\pi}^{(N-1)}}. \tag{11}$$

The Euclidean space structure associated to random walks can be interpreted in terms of the first-passage properties [16]. Indeed, we can consider the vector $\mathbf{e}_i = \{0, \ldots, 1_i, \ldots, 0\}$ that represents the node $i \in V$ in the canonical basis as a density function. Then, the squared norm (9) of the vector $\mathbf{e}_i$ gives the spectral representation of the first passage time to the node i from a node randomly chosen among all nodes of the graph accordingly to the stationary distribution π. The first passage time can be directly used in order to characterize the level of accessibility of the node i. The Euclidean distance (11) is the spectral representation of

the commute time, the expected number of steps required for a random walker starting at $i \in V$ to visit $j \in V$ and then to return back to i [18]. The scalar product (8) estimates the expected overlap of random paths towards the nodes i and j starting from a node randomly chosen in accordance with the stationary distribution of random walks π [16].

4 Spectra of Cities

In this section, we study the spectra

$$\rho(\lambda) = \sum_{k=1}^{N} \delta(\lambda - \lambda_k), \quad \lambda_k \in [0, 2], \tag{12}$$

of the normalized Laplace operator (6) defined on the connected, undirected spatial graphs of compact urban patterns. Spectra bring out the symmetries of graphs.

If we take many random numbers from an interval of all real numbers symmetric with respect to a unit and calculate the sample mean in each case, then the distribution of these sample means will be approximately normal in shape and centered at 1 provided the size of samples was large. The probability density function of a normal distribution then forms a symmetrical bell-shaped curve highest at the mean value indicating that in a random selection of the numbers around the mean have a higher probability of being selected than those far away from the mean. Maximizing information entropy among all distributions with known mean and variance, the normal distribution arises in many areas of statistics.

It is interesting to compare the empirical distributions of eigenvalues over the interval [0, 2] in the city spectra with the normal distribution centered at 1. In Fig. 1, we have shown a probability-probability plot of the normal distribution (on the horizontal axis) against the empirical distribution of eigenvalues in the city spectra. A random sample of the normal distribution, having size equal to the number of eigenvalues in the spectrum has been be generated, sorted ascendingly, and plotted against the response of the empirical distribution of city eigenvalues.

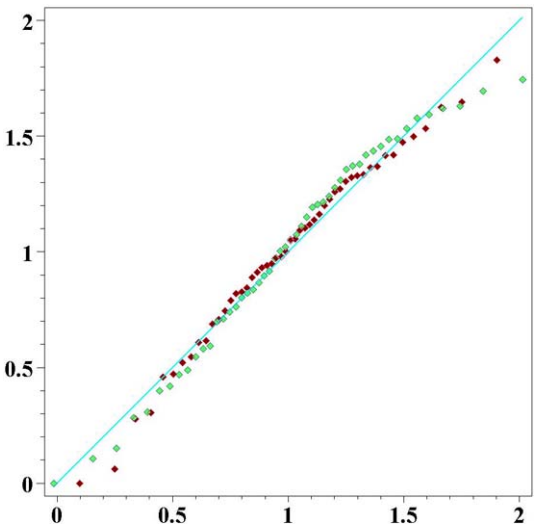

Fig. 1 The probability-probability plot of the normal distribution (on the horizontal axis) against the empirical distribution of eigenvalues in the city spectra of German medieval cities, Bielefeld and Rothenburg o.d.T. The coincidence line $y = x$ is set for a reference

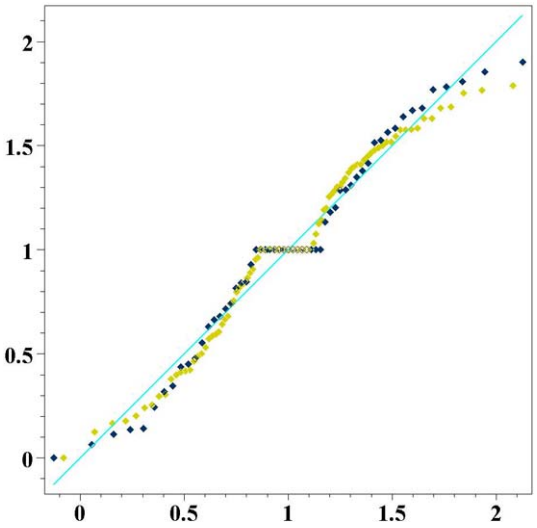

Fig. 2 The probability-probability plot of the normal distribution (on the horizontal axis) against the empirical distribution of eigenvalues in the spectra of the city canal networks in Venice and Amsterdam. The coincidence line $y = x$ is set for a reference

The spectra of all organic cities—the downtown of Bielefeld and the Rothenburg o.d.T. (see Fig. 1) are the examples—are akin to the Gaussian curve centered at 1.

The Fig. 2 shows the normal plot analogous to that given in Fig. 1, but for the empirical distribution of eigenvalues in the spectra of the city canal networks in Venice and Amsterdam. The spectra of canal maintained in the compact urban patterns of Venice and Amsterdam look also amazingly alike and are obviously tied to the normal distribution, although these canals had been founded in dissimilar geographical regions and intended to different purposes. While the Venetian canals mostly serve the function of transportation routs between the distinct districts of the gradually growing naval capital of the whole Mediterranean region, the concentric web of Amsterdam gratchen had been built in order to defend the city.

It is interesting to mention that the multiple eigenvalue $\lambda = 1$ would score a valuable fraction of all eigenvalues for the spatial graphs of modern cites. In this case, the resulting distribution of eigenvalues can essentially depart from any standard Gaussian curve of normal distributions (see the normal plot presented in Fig. 3).

It is remarkable that the spectral density distributions shown in Figs. 1–3 are dramatically different to those reported for the random graphs of Erdös and Rényi studied by [21, 22].

The classical Wigner semicircle distribution (see [23]) arises as the limiting distribution of eigenvalues of many random symmetric matrices as the size of the matrix approaches infinity [24]. In accordance to it, in random graphs, the nontrivial eigenvalues of their adjacency matrices cluster close to 1 [25, 26]. This fact remains true even for the spectra of scale-free random graphs with a power-law degree distribution that has been observed for the scale-free random tree-like graphs by [27]. In [28], the density distributions of eigenvalues for the Internet graph on the Autonomous Systems level had been presented. These distributions appear to be broad and have two symmetric maxima being similar to the spectral density distribution reported for random scale-free networks. The eigenvalues of the normalized Laplace operator in a random power-law graph also follow the semicircle law [29], whereas the spectrum of the adjacency matrix of a power-law graph obeys a power law [30].

In contrast to all of them, the spectral density distributions for compact urban patterns are either bell shaped, or have a sharp peak at $\lambda = 1$. City spectra reveal the profound structural

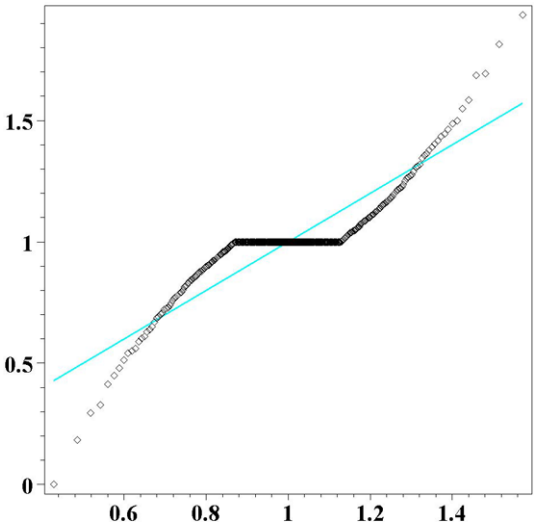

Fig. 3 The probability-probability plot of the normal distribution (on the horizontal axis) against the empirical distribution of eigenvalues of the spatial graph of Manhattan. The coincidence line $y = x$ is set for a reference

dissimilarity between urban networks and networks of other types studied before. This multiple eigenvalue appears due to twins nodes in the spatial graphs. Twins would arrive as the cliental nodes of star graphs being connected to the one and the same hub—star graph could represent the urban sprawl developments. They also can be found in the complete bipartite subgraphs that encode in spatial graphs the ideally regular street grids. These structures appear to be overrepresented in some compact urban patterns.

5 Thermodynamics of Urban Networks

The spectrum (12) is non-negative, and therefore we can investigate it by means of methods strongly inspired by statistical mechanics. The characteristic function,

$$\begin{aligned} Z(\beta) &= \int_0^\infty e^{-\beta\lambda}\rho(\lambda)d\lambda \\ &= \sum_{k=1}^{N} e^{-\beta\lambda_k}, \end{aligned} \tag{13}$$

(known as the canonical partition function) discriminates large eigenvalues in favor of smaller ones. The laziness parameter β determines the time scale in the random walk process (the mobility of random walkers).

For random walks defined on the undirected graphs, the density distributions of random walkers, $\sigma_i \geq 0$, $\sum_{i\in V}\sigma_i = 1$, play the role of the microscopic observables. A system is in equilibrium when its macroscopic observables have ceased to change with time, thus the stationary distribution of random walks $\pi = \psi_1^2$ can be naturally interpreted as the equilibrium state of the random walk process. Other microstates are described by the next eigenvectors.

The stationary distribution of random walks is the state of maximal probability, and therefore bringing up the concept of the canonical ensemble, it is possible to derive the probability $\Pr_k$ that random walkers could be found on the graph G in a certain microstate $\sigma_i^{(k)} = \psi_{k,i}^2$

belonging to the spectral value λ_k:

$$\Pr_k = Z^{-1}(\beta)\exp(-\beta\lambda_k). \tag{14}$$

It is worth to mention that since random walkers neither have masses, nor kinetic energy, they do not interact with each other and nontrivial expectations which can be found with the use of (13) characterize nothing else but certain structural properties of the graph itself.

5.1 Internal Energy of Urban Space

The averaged eigenvalue,

$$\begin{aligned}\langle\lambda\rangle &= Z(\beta)^{-1}\sum_{i=1}^{N}\lambda_i e^{-\beta\lambda_i}\\ &= -\partial_\beta \ln Z(\beta),\end{aligned} \tag{15}$$

held at a constant value of laziness parameter β can be interpreted as the microscopic definition of the thermodynamic variable corresponding to the internal energy in statistical mechanics.

Due to the complicated topology of streets and canals, the flows of random walkers exhibit spectral properties similar to that of a thermodynamic system characterized by a nontrivial internal energy. The principle of equipartition of energy in classical statistical mechanics gives the average values of individual components of the energy, such as the kinetic energy of a particular particle—it can be applied to any classical system in thermal equilibrium, no matter how complicated. In particular, the equipartition theorem states that each molecular quadratic degree of freedom receives $1/2kT = 1/(2\beta)$ of energy.

From Fig. 4, one can clearly see that at low mobility of random walkers ($\beta \ll 1$) the system of lazy random walks defined on the spatial graphs of compact urban patterns behaves as a system characterized by two quadratic degrees of freedom. While β increases,

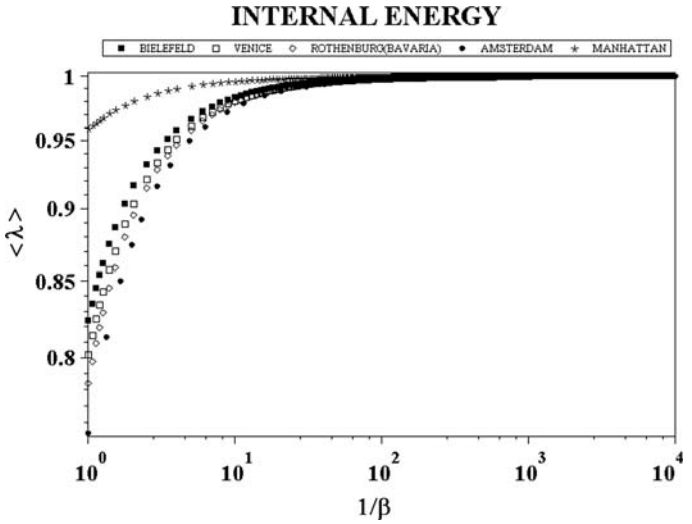

Fig. 4 The expected values of the "microscopic energy" (the averaged eigenvalues) are calculated for the spectra of compact urban patterns via the laziness of random walkers

more random walkers probably change their locations at each time step thus contributing into a pattern of motion characterized by one degree of freedom. The difference between the street layout patterns of the organic cities (Bielefeld, Rothenburg, canals of Amsterdam and Venice) and the street grid of Manhattan is revealed by the relative decrease of the internal energy as $\beta \to 1$. While in Manhattan, random walks remain to be almost 2-dimensional even at $\beta = 1$.

Taking the derivative of $\langle\lambda\rangle$ with respect to the parameter β in (15), we have

$$\frac{d\langle\lambda\rangle}{d\beta} = \langle\lambda\rangle^2 - \langle\lambda^2\rangle = -D^2(\lambda), \tag{16}$$

where $D^2(\lambda)$ is the variance, the measure of its statistical dispersion, indicating how the eigenvalues of the normalized Laplace operator are spread around the expected value $\langle\lambda\rangle$ tracing the variability of the eigenvalues. The standard deviation is then calculated by

$$\sigma = \sqrt{D^2(\lambda)}. \tag{17}$$

A large standard deviation indicates that the data points are far from the mean and a small standard deviation indicates that they are clustered closely around the mean (see Fig. 5).

The standard deviations of eigenvalues around the mean are almost insensitive to the mobility of random walkers being as twice as larger for organic cities than for the pattern planned in a regular grid (see Fig. 5).

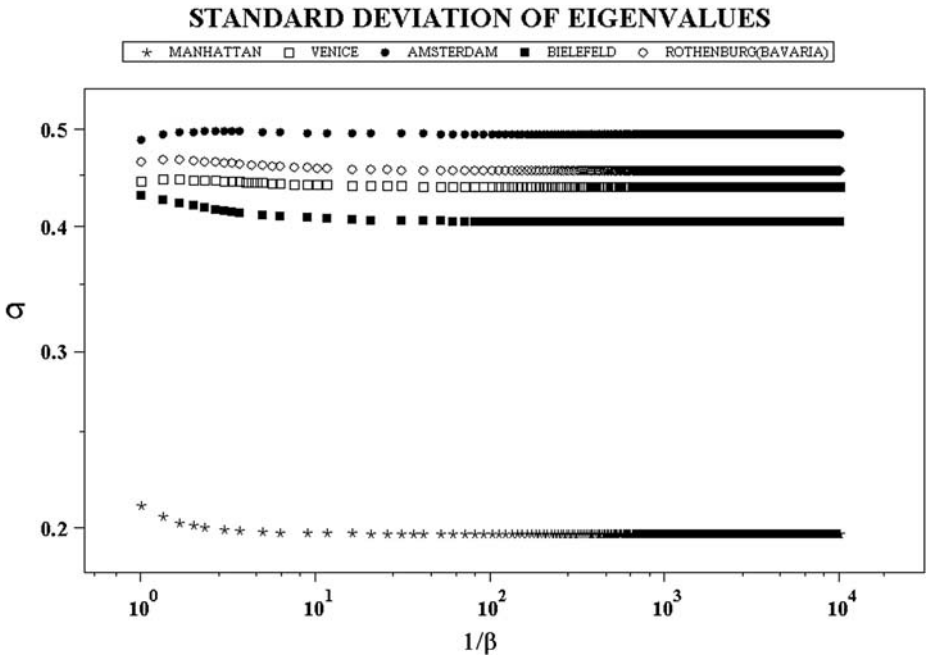

Fig. 5 The standard deviations of eigenvalues around the mean are calculated for the spectra of compact urban patterns via the laziness of random walkers

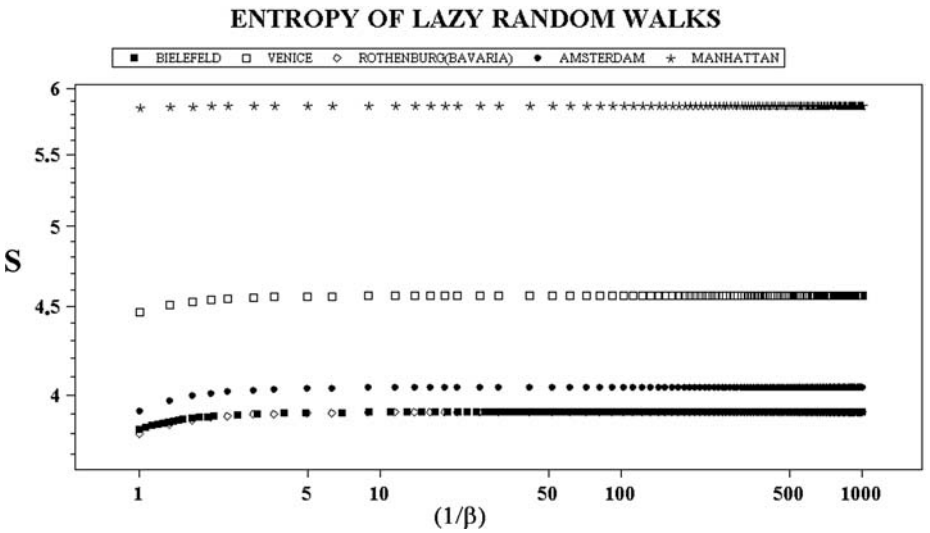

Fig. 6 The entropy of lazy random walks calculated for the spectra of compact urban patterns via the laziness of random walkers

5.2 Entropy of Urban Space

In thermodynamics, entropy accounts for the effects of irreversibility describing the number of possible observables in the system. For random walks defined on finite undirected graphs, its value,

$$S = -\sum_{k=1}^{N} \mathrm{Pr}_k \ln \mathrm{Pr}_k, \tag{18}$$

quantifies the probable number of density distributions of random walks which can be observed in the system before the stationary distribution π is achieved.

In Fig. 6, we have displayed the entropy curves versus temperature in the studied cities.

6 Directed and Interacting Transport Networks

Many transport networks are naturally abstracted as directed graphs.

Traffic within large cities is formally organized with marked driving directions creating one-way streets. It is well known empirically that the use of one-way streets would greatly improve traffic flow since the speed of traffic is increased and intersections are simplified.

Up to our knowledge, there is just a few works in so far devoted to the analysis of complex directed networks. Furthermore, the global transport network in the city usually consists of many different transportation modes which can be used alternatively by passengers while travelling (say, by trams, buses, subway, private vehicles, and by foot) at certain transport stations or elsewhere. Interactions between the individual transportation modes by means of passengers are responsible for the multiple complex phenomena we may daily observe on streets and while using the public transportation.

The spectral approach for directed graphs has not been as well developed as for undirected graph. Indeed, it is rather difficult if ever possible to define a unique self-adjoint operator on directed graphs.

In general, any node $i \in V$ in a directed graph $\vec{G}$ can have different number of in-neighbors and out-neighbors,

$$k_{\text{in}}(i) \neq k_{\text{out}}(i). \tag{19}$$

In particular, a node i is a *source* if $k_{\text{in}}(i) = 0$, $k_{\text{out}}(i) \neq 0$, and is a *sink* if $k_{\text{out}}(i) = 0$, $k_{\text{in}}(i) \neq 0$. If the graph has neither sources nor sinks, it is called strongly connected.

A recent investigation by [31] shows that directed networks often have very few short loops as compared to finite random graph models. In directed networks, the correlation between number of incoming and outgoing edges modulates the expected number of short loops—if the values $k_{\text{in}}(i)$ and $k_{\text{out}}(i)$ are not correlated, then the number of short loops is strongly reduced as compared to the case when both degrees are positively correlated.

6.1 Random Walks on Directed Graphs

Finite random walks are defined on a strongly connected directed graph $\vec{G}(V, \vec{E})$ as finite vertex sequences $\mathfrak{w} = \{v_0, \ldots, v_n\}$ (time forward) and $\mathfrak{w}' = \{v_{-n}, \ldots, v_0\}$ (time backward) such that each pair (v_{i-1}, v_i) of vertices adjacent either in $\mathfrak{w}$ or in $\mathfrak{w}'$ constitutes a directed edge $v_{i-1} \to v_i$ in $\vec{G}$.

A *time forward* random walk is defined by the transition probability matrix [32] P_{ij} for each pair of nodes $i, j \in \vec{G}$ by

$$P_{ij} = \begin{cases} 1/k_{\text{out}(i)}, & i \to j, \\ 0, & \text{otherwise}, \end{cases} \tag{20}$$

which satisfies the probability conservation property:

$$\sum_{j, i \to j} P_{ij} = 1. \tag{21}$$

The definition (20) can be naturally extended for weighted graphs [32] with $w_{ij} > 0$,

$$P_{ij} = \frac{w_{ij}}{\sum_{s \in V} w_{is}}. \tag{22}$$

Matrices (20) and (22) are real, but not symmetric and therefore have complex conjugated pairs of eigenvalues. For each pair of nodes $i, j \in \vec{G}$, the *forward* transition probability is given by $p_{ij}^{(t)} = (\mathbf{P}^t)_{ij}$ that is equal zero, if $\vec{G}$ does not contain a directed path from i to j.

Backwards time random walks are defined on the strongly connected directed graph $\vec{G}$ by the stochastic transition matrix

$$P_{ij}^{\star} = \begin{cases} 1/k_{\text{in}}(i), & j \to i, \\ 0, & \text{otherwise}, \end{cases} \tag{23}$$

satisfying *another* probability conservation property

$$\sum_{i, i \to j} P_{ij}^{\star} = 1. \tag{24}$$

It describes random walks unfolding backwards in time: should a random walker arrives at $t = 0$ at a node v_0, then

$$p_{ij}^{(-t)} = ((\mathbf{P}^{\star})^t)_{ij} \tag{25}$$

defines the probability that t steps *before* it had originated from a node j. The matrix element (25) is zero, provided there is no directed path from j to i in $\vec{G}$.

If $\vec{G}$ is strongly connected and *aperiodic*, the random walk converges [32–35] to the unique stationary distribution π given by the Perron vector, $\pi\mathbf{P} = \pi$. If the graph $\vec{G}$ is periodic, then the transition probability matrix $\mathbf{P}$ can have more than one eigenvalue with absolute value 1 [20]. The components of Perron's vector π can be normalized in such a way that $\sum_i \pi_i = 1$. The Perron vector for random walks defined on a strongly connected directed graph can have coordinates with exponentially small values [32].

Given an aperiodic strongly connected graph $\vec{G}$, a self-adjoint Laplace operator $L = L^{\top}$ can be defined [32] by setting

$$L_{ij} = \delta_{ij} - \frac{1}{2}\left(\pi^{1/2}\mathbf{P}\pi^{-1/2} + \pi^{-1/2}\mathbf{P}^{\top}\pi^{1/2}\right)_{ij}, \tag{26}$$

where π is a diagonal matrix with entries π_i. The matrix (26) is symmetric and has real non-negative eigenvalues $0 = \lambda_1 < \lambda_2 \leq \cdots \leq \lambda_N$ and real eigenvectors.

It can be easily proven [36] that the Laplace operator (26) defined on the aperiodic strongly connected graph $\vec{G}$ is equivalent to the Laplace operator defined on a *symmetric undirected weighted* graph G_w on the same vertex set with weights defined by

$$w_{ij} = \pi_i P_{ij} + \pi_j P_{ji}. \tag{27}$$

6.2 Bi-orthogonal Decomposition of Random Walks Defined on Strongly Connected Directed Graphs

In order to define the self-adjoint Laplace operator (26) on aperiodic strongly connected directed graphs, we have to know the stationary distributions π of random walkers. Even if π exists for a given directed graph $\vec{G}$, it can be evaluated usually only numerically in polynomial time [33]. Stationary distributions on aperiodic general directed graphs are not so easy to describe since they are typically *non-local* in sense that each coordinate π_i would depend upon the entire subgraph (the number of spanning arborescences of $\vec{G}$ rooted at i [33]), but not on the local connectivity property of a node itself like it was the case for undirected graphs. Furthermore, if the greatest common divisor of its cycle lengths in $\vec{G}$ exceeds 1, then the transition probability matrices (20) and (23) can have several eigenvectors belonging to the largest eigenvalue 1, so that the definition (26) of Laplace operator seems to be questionable.

Given a strongly connected directed graph $\vec{G}$ specified by the adjacency matrix $\mathbf{A}_{\vec{G}} \neq \mathbf{A}_{\vec{G}}^{\top}$, we consider two random walks operators. A first transition operator represented by the matrix

$$\mathbf{P} = \mathbf{D}_{\text{out}}^{-1}\mathbf{A}_{\vec{G}}, \tag{28}$$

in which $\mathbf{D}_{\text{out}}$ is a diagonal matrix with entries $k_{\text{out}}(i)$, describes the *time forward* random walks of the nearest neighbor type defined on $\vec{G}$. Given a time forward vertex sequence $\mathfrak{w}$ rooted at $i \in \vec{G}$, the matrix element P_{ij} gives the probability that $j \in \vec{G}$ is the vertex next to

i in $\mathfrak{w}$. A second transition operator, $\mathbf{P}^\star$, is dynamically conjugated to (28),

$$\begin{aligned}\mathbf{P}^\star &= \mathbf{D}_{\text{in}}^{-1}\mathbf{A}_{\vec{G}}^{\top} \\ &= \mathbf{D}_{\text{in}}^{-1}\mathbf{P}^{\top}\mathbf{D}_{\text{out}},\end{aligned} \tag{29}$$

where $\mathbf{D}_{\text{in}}$ is a diagonal matrix with entries $k_{\text{in}}(i)$. The transition operator (29) describes random walks over time backward vertex sequences $\mathfrak{w}'$.

It is worth to mention that on undirected graphs $\mathbf{P}^\star \equiv \mathbf{P}$, since $k_{\text{in}}(i) = k_{\text{out}}(i)$ for $\forall i \in \vec{G}$ and $\mathbf{A}_G = \mathbf{A}_G^{\top}$. While on directed graphs, $\mathbf{P}^\star$ is related to $\mathbf{P}$ by the transformation

$$\mathbf{P} = \mathbf{D}_{\text{out}}^{-1}\left(\mathbf{P}^\star\right)^{\top}\mathbf{D}_{\text{in}}, \tag{30}$$

so that these operators are not symmetric, in general $\mathbf{P}^{\top} \neq \mathbf{P}^\star$.

We can define two different measures

$$\mu_+ = \sum_j \deg_{\text{out}}(j)\delta(j), \qquad \mu_- = \sum_j \deg_{\text{in}}(j)\delta(j) \tag{31}$$

associated with the *out*- and *in*-degrees of nodes of the directed graph. In accordance to (31), we define two Hilbert spaces $\mathcal{H}_+$ and $\mathcal{H}_-$ corresponding to the spaces of square summable functions, $\ell^2(\mu_+)$ and $\ell^2(\mu_-)$, by setting the norms as

$$\|x\|_{\mathcal{H}_\pm} = \sqrt{\langle x, x\rangle}_{\mathcal{H}_\pm},$$

where $\langle\cdot,\cdot\rangle_{\mathcal{H}_\pm}$ denotes the inner products with respect to measures (31). Then a function $f(j)$ defined on the set of graph vertices is $f_{\mathcal{H}_-}(j) \in \mathcal{H}_-$ if transformed by

$$f_{\mathcal{H}_-}(j) \to J_- f(j) \equiv {\mu_-}_j^{-1/2} f(j) \tag{32}$$

and $f_{\mathcal{H}_+}(j) \in \mathcal{H}_+$ while being transformed accordingly to

$$f_{\mathcal{H}_+}(j) \to J_+ f(j) \equiv {\mu_+}_j^{-1/2} f(j). \tag{33}$$

The obvious advantage of the measures (31) against the natural counting measure $\mu_0 = \sum_{i\in V}\delta_i$ is that the matrices of the transition operators P and $P^\star$ are transformed under the change of measures as

$$P_\mu = J_+^{-1} P J_-, \qquad P_\mu^\star = J_-^{-1} P^\star J_+, \tag{34}$$

and become adjoint,

$$\begin{aligned}\left(P_\mu\right)_{ij} &= \frac{A_{\vec{G}ij}}{\sqrt{k_{\text{out}}(i)}\sqrt{k_{\text{in}}(j)}}, \\ \left(P_\mu^\star\right)_{ij} &\equiv \left(P_\mu^{\top}\right)_{ij} = \frac{A_{\vec{G}ij}^{\top}}{\sqrt{k_{\text{in}}(i)}\sqrt{k_{\text{out}}(j)}}.\end{aligned} \tag{35}$$

It is also important to note that

$$P_\mu : \mathcal{H}_- \to \mathcal{H}_+ \quad \text{and} \quad P_\mu^\star : \mathcal{H}_+ \to \mathcal{H}_-.$$

We obtain the singular value dyadic expansion (*biorthogonal decomposition* introduced in [37, 38]) for the transition operator:

$$\mathbf{P}_\mu = \sum_{s=1}^{N} \Lambda_s \varphi_{si} \psi_{si} \equiv \sum_{s=1}^{N} \Lambda_s |\varphi_s\rangle\langle\psi_s|, \tag{36}$$

where $0 \le \Lambda_1 \le \cdots \le \Lambda_N$ and the functions $\varphi_k \in \mathcal{H}_+$ and $\psi_k \in \mathcal{H}_-$ are related by the Karhunen-Loève *dispersion* [39, 40],

$$\mathbf{P}_\mu \varphi_s = \Lambda_s \psi_s \tag{37}$$

satisfying the orthogonality condition:

$$\langle \varphi_s, \varphi_{s'} \rangle_{\mathcal{H}_+} = \langle \psi_{s'}, \psi_s \rangle_{\mathcal{H}_-} = \delta_{s's}. \tag{38}$$

Since the operators P_μ and $P_\mu^\top$ act between different Hilbert spaces, the solution of one eigenvalue problem is not enough in order to determine their eigenvectors φ_s and ψ_s [41]. Instead, two equations have to be solved,

$$\begin{cases} \mathbf{P}_\mu \varphi = \Lambda \psi, \\ \mathbf{P}_\mu^\top \psi = \Lambda \varphi, \end{cases} \tag{39}$$

or, equivalently,

$$\begin{pmatrix} 0 & \mathbf{P}_\mu \\ \mathbf{P}_\mu^\top & 0 \end{pmatrix} \begin{pmatrix} \varphi \\ \psi \end{pmatrix} = \Lambda \begin{pmatrix} \varphi \\ \psi \end{pmatrix}. \tag{40}$$

The latter equation allows for a graph-theoretical interpretation. The block anti-diagonal operator matrix in the left hand side of (40) describes random walks defined on a bipartite graph. Bipartite graphs contain two disjoint sets of vertices such that no edge has both end-points in the same set. However, in (40), both sets are formed by one and the same nodes of the original graph $\vec{G}$ on which two different random walk processes specified by the operators P_μ and $P_\mu^\top$ are defined.

It is obvious that any solution of (40) is also a solution of the system

$$U\varphi = \Lambda^2 \varphi, \qquad V\psi = \Lambda^2 \psi, \tag{41}$$

in which $U \equiv \mathbf{P}_\mu^\top \mathbf{P}_\mu$ and $V \equiv \mathbf{P}_\mu \mathbf{P}_\mu^\top$, although the converse is not necessarily true. The self-adjoint nonnegative operators $U : \mathcal{H}_- \to \mathcal{H}_-$ and $V : \mathcal{H}_+ \to \mathcal{H}_+$ share one and the same set of eigenvalues $\Lambda^2 \in [0, 1]$, and the orthonormal functions $\{\varphi_k\}$ and $\{\psi_k\}$ constitute the orthonormal basis for the Hilbert spaces $\mathcal{H}_+$ and $\mathcal{H}_-$ respectively. The Hilbert-Schmidt norm of both operators,

$$\operatorname{tr}\left(P_\mu^\top P_\mu\right) = \operatorname{tr}\left(P_\mu P_\mu^\top\right) = \sum_{s=1}^{N} \Lambda_s^2 \tag{42}$$

is a *global characteristic* of the directed graph.

Provided the random walks are defined on a strongly connected directed graph $\vec{G}$, let us consider the functions $\rho^{(t)}(s) \in [0, 1] \times \mathbb{Z}_+$ representing the probability for finding a random walker at the node s, at time t. A random walker located at the source node s can reach

the node s' through either nodes. Being transformed in accordance to (32) and (33), these function takes the following forms: $(\rho_s^{(t)})_{\mathcal{H}_-} = \mu_-^{-1/2}\rho^{(t)}(s)$ and $(\rho_s^{(t)})_{\mathcal{H}_+} = \mu_+^{-1/2}\rho^{(t)}(s)$. Then, the self-adjoint operators $U : \mathcal{H}_- \to \mathcal{H}_-$ and $V : \mathcal{H}_+ \to \mathcal{H}_+$ with the matrix elements

$$\begin{aligned} U_{ss'} &= \frac{1}{\sqrt{k_{\text{out}}(s)k_{\text{in}}(s')}} \sum_{i\in\vec{G}} \frac{A^{\top}_{\vec{G}is} A_{\vec{G}is'}}{\sqrt{k_{\text{out}}(i)k_{\text{in}}(i)}}, \\ V_{s's} &= \frac{1}{\sqrt{k_{\text{out}}(s')k_{\text{in}}(s)}} \sum_{i\in\vec{G}} \frac{A_{\vec{G}s'i} A^{\top}_{\vec{G}si}}{\sqrt{k_{\text{out}}(i)k_{\text{in}}(i)}} \end{aligned} \tag{43}$$

define the dynamical system

$$\begin{cases} \sum_{s\in\vec{G}} \left(\rho_s^{(t)}\right)_{\mathcal{H}_-} U_{ss'} = \left(\rho_{s'}^{(t+2)}\right)_{\mathcal{H}_-}, \\ \sum_{s'\in\vec{G}} \left(\rho_{s'}^{(t)}\right)_{\mathcal{H}_+} V_{s's} = \left(\rho_s^{(t+2)}\right)_{\mathcal{H}_+}. \end{cases} \tag{44}$$

The spectral properties of the self-adjoint operators U and V driving two Markov processes on strongly connected directed graphs and sharing the same non-negative eigenvalues $\Lambda_s^2 \in [0, 1]$ can be analyzed separately by the method of characteristic functions as we did in the Sect. 5.

The self-adjoint operators U and V describe correlations between flows of random walkers entering and leaving nodes in a directed graph—the strongest correlations are labelled by the largest eigenvalues Λ_k^2, $k = 1, \ldots, N$.

6.3 Self-adjoint Operators for Interacting Networks

The bi-orthogonal decomposition can also be implemented in order to determine coherent segments of two or more interacting networks defined on one and the same set of nodes V, $|V| = N$.

Given two different strongly connected weighted directed graphs $\vec{G}_1$ and $\vec{G}_2$ specified on the same set of N vertices by the non-symmetric adjacency matrices $\mathbf{A}^{(1)}$, $\mathbf{A}^{(2)}$, which entries are the edge weights, $w_{ij}^{(1,2)} \geq 0$, then the four transition operators of random walks can be defined on both networks as

$$\mathbf{P}^{(\alpha)} = \left(\mathbf{D}_{\text{out}}^{(\alpha)}\right)^{-1} \mathbf{A}^{(\alpha)}, \quad \left(\mathbf{P}^{(\alpha)}\right)^{\star} = \left(\mathbf{D}_{\text{in}}^{(\alpha)}\right)^{-1} \mathbf{A}^{(\alpha)}, \quad \alpha = 1, 2, \tag{45}$$

where $\mathbf{D}_{\text{out/in}}$ are the diagonal matrices with the following entries:

$$k_{\text{out}}^{(\alpha)}(j) = \sum_{i,j\to i} w_{ji}^{(\alpha)}, \quad k_{\text{in}}^{(\alpha)}(j) = \sum_{i,i\to j} w_{ij}^{(\alpha)}, \quad \alpha = 1, 2. \tag{46}$$

We can define 4 different measures,

$$\begin{aligned} \mu_-^{(1)} &= \sum_j k_{\text{out}}^{(1)}(j)\delta(j), \qquad \mu_+^{(1)} = \sum_j k_{\text{in}}^{(1)}(j)\delta(j), \\ \mu_-^{(2)} &= \sum_j k_{\text{out}}^{(2)}(j)\delta(j), \qquad \mu_+^{(2)} = \sum_j k_{\text{in}}^{(2)}(j)\delta(j), \end{aligned} \tag{47}$$

and four Hilbert spaces $\mathcal{H}_{\pm}^{(\alpha)}$ associated with the spaces of square summable functions, $\ell^2(\mu_{\pm}^{(\alpha)})$, $\alpha = 1, 2$.

Then the transitions operators $P_{\mu}^{(\alpha)} : \mathcal{H}_{-}^{(\alpha)} \to \mathcal{H}_{-}^{(\alpha)}$ and $(P_{\mu}^{(\alpha)})^{\star} : \mathcal{H}_{+}^{(\alpha)} \to \mathcal{H}_{+}^{(\alpha)}$ adjoint with respect to the measures $\mu_{\pm}^{(\alpha)}$ are defined by the following matrices:

$$\begin{aligned} \left(P_{\mu}^{(\alpha)}\right)_{ij} &= \frac{{A_{\tilde{G}}^{(\alpha)}}_{ij}}{\sqrt{k_{\text{out}}^{(\alpha)}(i)}\sqrt{k_{\text{in}}^{(\alpha)}(j)}}, \\ \left(P_{\mu}^{(\alpha)}\right)_{ij}^{\star} &= \frac{{A^{(\alpha)\top}_{\tilde{G}}}_{ij}}{\sqrt{k_{\text{in}}^{(\alpha)}(i)}\sqrt{k_{\text{out}}^{(\alpha)}(j)}}. \end{aligned} \tag{48}$$

The spectral analysis of the above operators requires that four equations be solved:

$$\begin{cases} \mathbf{P}_{\mu}^{(\alpha)} \varphi^{(\alpha)} = \Lambda^{(\alpha)} \psi^{(\alpha)}, \\ \mathbf{P}_{\mu}^{(\alpha)\top} \psi^{(\alpha)} = \Lambda^{(\alpha)} \varphi^{(\alpha)}, \end{cases} \tag{49}$$

where $\alpha = 1, 2$ as usual.

Any solution $\{\varphi^{(\alpha)}, \psi^{(\alpha)}\}$ of the system (49), up to the possible partial isometries,

$$\mathbf{G}^{(\alpha)} \varphi^{(\alpha)} = \psi^{(\alpha)}, \tag{50}$$

also satisfies the system

$$\begin{aligned} \mathbf{P}_{\mu}^{(2)\top} \mathbf{P}_{\mu}^{(1)} \mathbf{P}_{\mu}^{(1)\top} \mathbf{P}_{\mu}^{(2)} \psi^{(2)} &= \left(\Lambda^{(1)} \Lambda^{(2)}\right)^2 \psi^{(2)}, \\ \mathbf{P}_{\mu}^{(1)\top} \mathbf{P}_{\mu}^{(2)} \mathbf{P}_{\mu}^{(2)\top} \mathbf{P}_{\mu}^{(1)} \psi^{(1)} &= \left(\Lambda^{(1)} \Lambda^{(2)}\right)^2 \psi^{(1)}, \\ \mathbf{P}_{\mu}^{(1)} \mathbf{P}_{\mu}^{(1)\top} \mathbf{P}_{\mu}^{(2)} \mathbf{P}_{\mu}^{(2)\top} \varphi^{(1)} &= \left(\Lambda^{(1)} \Lambda^{(2)}\right)^2 \varphi^{(1)}, \\ \mathbf{P}_{\mu}^{(2)} \mathbf{P}_{\mu}^{(2)\top} \mathbf{P}_{\mu}^{(1)} \mathbf{P}_{\mu}^{(1)\top} \varphi^{(2)} &= \left(\Lambda^{(1)} \Lambda^{(2)}\right)^2 \varphi^{(2)}, \end{aligned} \tag{51}$$

in which $(\Lambda^{(1)} \Lambda^{(2)})^2 \in [0, 1]$. Operators in the l.h.s of the system (51) describe correlations between flows of random walkers which go through vertices following the links of either networks. Their spectrum can also be investigated by the methods discussed in the previous subsection.

It is convenient to represent the self-adjoint operators from the l.h.s. of (51) by the closed directed paths shown in the diagram in Fig. 7. Being in the self-adjoint products of transition

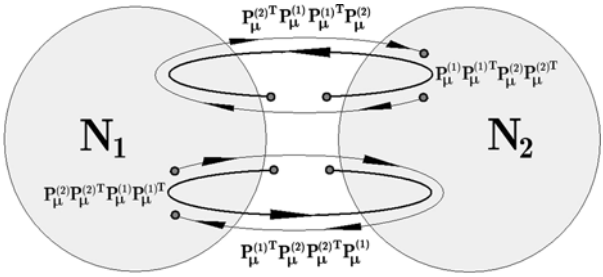

Fig. 7 Self-adjoint operators for two interacting networks sharing the same set of nodes

operators, $P_{\mu}^{(\alpha)}$ corresponds to the flows of random walkers which depart from either networks, and $P_{\mu}^{(\alpha)\top}$ is for those which arrive at the network α. From Fig. 7 , it is clear that the self-adjoint operators in (51) represent all possible closed trajectories visiting both networks $\mathbf{N}_1$ and $\mathbf{N}_2$.

In general, given a complex system consisting of $n > 1$ interacting networks operating on the same set of nodes, we can define 2^n self-adjoint operators related to the different modes of random walks. Then the set of network nodes can be separated into a number of essentially correlated segments with respect to each of self-adjoint operators.

7 Conclusion

In the present paper, we have developed a self-consistent approach to complex transport networks based on the use of Markov chains defined on their graph representations.

Flows of pedestrians, private vehicles, and public transportation through the city are dependent on one another and have to be organized in a network setting.

We have shown that any strongly connected directed graph $\vec{G}$ can be considered as a bipartite graph with respect to the in- and out-connectivity of nodes. The bi-orthogonal decomposition of random walks is then used in order to define the self-adjoint operators on directed graphs describing correlations between flows of random walkers which arrive at and leave the nodes. These self-adjoint operators share the non-negative real spectrum of eigenvalues, but different orthonormal sets of eigenvectors. The global characteristics of the directed graph and its components can be obtained from the spectral properties of the self-adjoint operators.

The approach we have discussed in the present paper helps to define an equilibrium state for complex transport networks and investigate its properties.

Acknowledgement The work has been supported by the Volkswagen Foundation (Germany) in the framework of the project: "Network formation rules, random set graphs and generalized epidemic processes" (Contract no Az.: I/82 418).

References

1. Braess, D.: Über ein Paradoxon aus der Verkehrsplannung. Unternehmensforschung **12**, 258–268 (1968)
2. Kolata, G.: What if they closed the 42nd Street and nobody noticed? The New York Times, Dec. 25 (1990)
3. Alexanderson, G.L.: Bull. Am. Math. Soc. **43**, 567–573 (2006)
4. Hillier, B., Hanson, J.: The Social Logic of Space. Cambridge University Press, Cambridge (1984). ISBN 0-521-36784-0
5. Hillier, B.: Space is the Machine: A Configurational Theory of Architecture. Cambridge University Press, Cambridge (1999). ISBN 0-521-64528-X
6. Rosvall, M., Trusina, A., Minnhagen, P., Sneppen, K.: Phys. Rev. Lett. **94**, 028701 (2005)
7. Cardillo, A., Scellato, S., Latora, V., Porta, S.: Phys. Rev. E **73**, 066107 (2006)
8. Porta, S., Crucitti, P., Latora, V.: Physica A **369**, 853 (2006)
9. Scellato, S., Gardillo, A., Latora, V., Porta, S.: Eur. Phys. J. B **50**, 221 (2006)
10. Crucitti, P., Latora, V., Porta, S.: Chaos **16**, 015113 (2006)
11. Volchenkov, D., Blanchard, Ph.: Phys. Rev. E **75**(2) (2007)
12. Volchenkov, D., Blanchard, Ph.: Physica A **387**(10), 2353–2364 (2008). doi:10.1016/j.physa.2007.11.049
13. Gross, D., Harris, C.M.: Fundamentals of Queueing Theory. Wiley, New York (1998)
14. Backus, B.T., Oruç, I.: J. Vis. **5**(11), 1055–1069 (2005)
15. Biggs, N.: Permutation Groups and Combinatorial Structures. Cambridge University Press, Cambridge (1979)

16. Blanchard, Ph., Volchenkov, D.: Intelligibility and first passage times in complex urban networks. Proc. R. Soc. A **464**, 2153–2167 (2008). doi:10.1098/rspa.2007.0329
17. Lagrange, J.-L.: Uvres, vol. 1, pp. 72–79. Gauthier-Villars, Paris (1867) (in French)
18. Lovász, L.: Combinatorics, Paul Erdös is Eighty. Bolyai Society Mathematical Studies, vol. 2, pp. 1–46. Bolyai Mathematical Society, Keszthely (1993)
19. Aldous, D.J., Fill, J.A.: Reversible Markov chains and random walks on graphs (in preparation). See http://www.stat.berkeley.edu/waldous/RWG/book.html
20. Chung, F.: Lecture Notes on Spectral Graph Theory. AMS, Providence (1997)
21. Farkas, I.J., Derényi, I., Barabási, A.-L., Vicsek, T.: Phys. Rev. E **64**, 026704 (2001)
22. Farkas, I., Derényi, I., Jeong, H., Neda, Z., Oltvai, Z.N., Ravasz, E., Schubert, A., Barabási, A.-L., Vicsek, T.: Physic A **314**, 25 (2002)
23. Abramowitz, M., Stegun, I.A. (eds.): Handbook of Mathematical Functions with Formulas, Graphs, and Mathematical Tables. Dover, New York (1972)
24. Sinai, Ya.G., Soshnikov, A.B.: Funct. Anal. Appl. **32**(2), 114–131 (1998)
25. Arnold, L.: Z. Wahrscheinlichkeitstheorie und Verw. Gebiete **19**, 191–198 (1971)
26. Alon, N., Krivelevich, M., Vu, V.H.: Isr. J. Math. **131**, 259–267 (2002)
27. Dorogovtsev, S.N., Goltsev, A.V., Mendes, J.F.F., Samukhin, A.N.: Phys. Rev. E **68**, 046109 (2003)
28. Eriksen, K.A., Simonsen, I., Maslov, S., Sneppen, K.: Phys. Rev. Lett. **90**(14), 148701 (2003)
29. Chung, F., Lu, L., Vu, V.: Proc. Natl. Acad. Sci. USA **100**(11), 6313–6318 (2003). Published online doi:10.1073/pnas.0937490100
30. Bollobás, B., Riordan, O.: Mathematical results on scale-free random graphs. In: Handbook of Graphs and Networks. Wiley, New York (2002)
31. Bianconi, G., Gulbahce, N., Motter, A.E.: Local structure of directed networks, 27 July 2007. E-print arXiv:0707.4084 [cond-mat.dis-nn]
32. Chung, F.: Ann. Comb. **9**, 1–19 (2005)
33. Lovász, L., Winkler, P.: Mixing of random walks and other diffusions on a graph. In: Surveys in Combinatorics, Stirling. London Math. Soc. Lecture Note Ser., vol. 218, 119–154. Cambridge Univ. Press, Cambridge (1995)
34. Björner, A., Lovász, L., Shor, P.: Eur. J. Comb. **12**, 283–291 (1991)
35. Björner, A., Lovász, L.: J. Algebr. Comb. **1**, 305–328 (1992)
36. Butler, S.: Electron. J. Linear Algebra **16**, 90 (2007)
37. Aubry, N., Guyonnet, R., Lima, R.: J. Stat. Phys. **64**, 683–739 (1991)
38. Aubry, N.: Theor. Comput. Fluid Dyn. **2**, 339–352 (1991)
39. Karhunen, K.: Ann. Acad. Sci. Fenn. A **1** (1944)
40. Loève, M.: Probability Theory. van Nostrand, New York (1955)
41. Aubry, N., Lima, L.: Spatio-temporal symmetries. Preprint CPT-93/P. 2923, Centre de Physique Theorique, Luminy, Marseille, France (1993)